Mon. Not. R. Astron. Soc. **000**, 000–000 (0000) Printed 1 February 2008 (MN LATEX style file v2.2)

Dynamical friction force exerted on spherical bodies

O. Esquivel⋆ and B. Fuchs
Astronomisches Rechen-Institut am Zentrum für Astronomie der Universität Heidelberg, Mönchhofstraße 12-14, 69120 Heidelberg, Germany

1 February 2008

ABSTRACT
We present a rigorous calculation of the dynamical friction force exerted on a spherical massive perturber moving through an infinite homogenous system of field stars. By calculating the shape and mass of the polarization cloud induced by the perturber in the background system, which decelerates the motion of the perturber, we recover Chandrasekhar's drag force law with a modified Coulomb logarithm. As concrete examples we calculate the drag force exerted on a Plummer sphere or a sphere with the density distribution of a Hernquist profile. It is shown that the shape of the perturber affects only the exact form of the Coulomb logarithm. The latter converges on small scales, because encounters of the test and field stars with impact parameters less than the size of the massive perturber become inefficient. We confirm this way earlier results based on the impulse approximation of small angle scatterings.

Key words: methods: analytical – galaxies: kinematics and dynamics

1 INTRODUCTION

The determination of the dynamical friction force exerted by a gravitating system of background stars on a test star moving through the system is one of the classical problems of stellar dynamics. In his seminal paper Chandrasekhar (1943) envisaged the scenario of a sequence of consecutive gravitational two–body encounters of test and field stars in order to calculate the drag force (cf. Hénon 1973 for a modern presentation). In an alternative approach Marochnik (1968) and Kalnajs (1972) determined the collective response of the background medium to a moving massive perturber which manifests itself as a polarization cloud decelerating the perturber. The dynamical friction force law derived in this way is precisely identical to Chandrasekhar's force law, if the mass of an individual field star can be neglected against the mass of the perturber. The latter is to be expected whenever the background can be treated as a gravitating continuum.

The applications of Chandrasekhar's formula covered a wide field, ranging from calculations of the dynamical friction and diffusion coefficients of the Fokker-Planck equation, which is used to describe the internal dynamics of star clusters, to determinations of the sinking rates of satellite galaxies which are accreted by massive galaxies. The literature on these subjects has become so extensive over the years that we do not attempt any detailed review here, because this would be beyond the scope of this paper. In the context of the sinking satellite problem most of the efforts concentrated on adapting the original concept of an infinite homogeneous background of field stars on isotropic straight–line orbits to geometries and kinematics appropriate for the discs and haloes of spiral galaxies. Moreover, the finite size of the perturbing body was taken into account. White (1976) followed Chandrasekhar's concept of a sequence of two–body encounters of field and test stars and considered a sequence of deflections of field stars by a moving spherical body. Technically the deflections were calculated using the impulse approximation of small angle scatterrings. The principal result was a modification of the Coulomb logarithm so that it does not diverge anymore at small scales, because gravitational encounters at impact parameters smaller than the size of the perturbing body become ineffective.

In this paper we present a rigorous calculation of the dynamical friction force exerted by an infinite homogenous background on a spherical massive body using the wave–mechanical method of Marochnik (1968) and Kalnajs (1972). This approach is topically closely related to studies of the exchange of angular and linear momentum in stellar systems (Lynden-Bell & Kalnajs 1972, Dekker 1974, Tremaine & Weinberg 1984, Fuchs 2004) or in plasmas (Stix 1992). It is shown in section 4 below that the shape of the perturber affects only the exact form of the Coulomb logarithm. As concrete examples we calculate the drag force exerted on a Plummer sphere and on a sphere with the density distribution of a Hernquist (1990) profile, respectively, and compare this with the drag force exerted on a point mass.

⋆ Fellow of IMPRS for Astronomy and Cosmic Physics, Heidelberg

2 INDUCED POLARIZATION CLOUDS

We assume an infinite homogenous distribution of field stars on isotropic straight–line orbits. The response of the system of background stars to the perturbation due to a massive perturber is determined by solving the linearized Boltzmann equation

$$\frac{\partial f_1}{\partial t} + \sum_{i=1}^{3} \mathrm{v_i} \frac{\partial f_1}{\partial \mathrm{x_i}} - \frac{\partial \Phi_1}{\partial \mathrm{x_i}} \frac{\partial f_0}{\partial \mathrm{v_i}} = 0\,, \tag{1}$$

where Φ_1 denotes the gravitational potential of the perturber and f_1 is the induced perturbation of the distribution function of the field stars in phase space. The unperturbed distribution function is described by f_0. The solution of the Boltzmann equation is greatly facilitated by considering Fourier transforms of the perturbations of the distribution function and the potential, respectively,

$$f_{\omega,\mathbf{k}};\ \Phi_{\omega,\mathbf{k}} \exp i[\omega t + \mathbf{k}\cdot\mathbf{x}]\,, \tag{2}$$

where ω and $\mathbf{k}$ denote the frequency and wave vector of the Fourier components. Without loss of generality the spatial coordinates $\mathrm{x_i}$ and the corresponding velocity components $\mathrm{v_i}$ can be oriented with one axis parallel to the direction of the wave vector. The Boltzmann equation (1) takes then the form

$$\omega f_{\omega,\mathbf{k}} + \upsilon k f_{\omega,\mathbf{k}} - k\Phi_{\omega,\mathbf{k}} \frac{\partial f_0}{\partial \upsilon} = 0 \tag{3}$$

with $k = |\mathbf{k}|$ and υ denoting the velocity component parallel to $\mathbf{k}$. Equation (3) has been integrated over the two velocity components perpendicular to $\mathbf{k}$. In the following we assume for the field stars always a Gaussian velocity distribution function, or specifically in eq. (3)

$$\frac{\partial f_0}{\partial \upsilon} = -\frac{\upsilon}{\sigma^2} \frac{n_\mathrm{b}}{\sqrt{2\pi}\sigma} e^{-\frac{\upsilon^2}{2\sigma^2}}\,, \tag{4}$$

where n_b denotes the spatial density of the field stars. We find then the solution of the Fourier transformed Boltzmann equation

$$f_{\omega,\mathbf{k}} = -\frac{k\upsilon}{\omega + k\upsilon} \frac{n_\mathrm{b}}{\sqrt{2\pi}\sigma^3} e^{-\frac{\upsilon^2}{2\sigma^2}} \Phi_{\omega,\mathbf{k}}\,. \tag{5}$$

Integrating eq. (5) over the υ–velocity leads to the density distribution of the induced polarization cloud. This has been calculated here without taking into account the self–gravity of the background medium. Fuchs (2004) has shown that in linear approximation the effects of self–gravity can be described by another linearized Boltzmann equation of the form of eq. (1) where Φ_1 denotes then the gravitational potential of the density perturbation of the background medium. In a self–gravitating system the density perturbations are the sources of the potential perturbations so that the density - potential pair has to fulfill the Poisson equation. The solution of the combined Boltzmann and Poisson equations describes simply the Jeans collapse of the background medium on scales larger than the Jeans length. In real stellar systems or dark haloes their Jeans length will be always larger than the size of the system, because otherwise the system would have collapsed to smaller sizes. Since the polarization cloud is contained within the system, self–gravity is not important for its dynamics.

Of course real self–gravitating systems are not homogeneous, but their density falls off radially. Moreover, their phase space distribution is more complicated than an isothermal Gaussian velocity distribution. In such systems a moving perturber can incite large scale perturbations which contribute to the dynamical friction of the perturber as well (Tremaine & Weinberg 1984, Colpi et al. 1999). Obviously these effects cannot be described by the simplified model adopted here. However, Colpi et al. (1999) among others have shown, that the drag by the localized polarization cloud on the moving perturber, which we treat here, is the principal effect.

3 POTENTIALS OF THE PERTURBING BODIES

For reference reasons we include in our analysis also the potential of a point mass, which moves with the velocity $\mathrm{v_0}$ along the y–axis,

$$\Phi_1 = -\frac{Gm}{\sqrt{\mathrm{x}^2 + (\mathrm{y} - \mathrm{v_0}t)^2 + \mathrm{z}^2}}\,. \tag{6}$$

Its Fourier-Transform can be calculated using formulae (3.754) and (6.561) of Gradshteyn & Rhyzik (2000) as

$$\Phi_\mathbf{k} = -\frac{Gm}{2\pi^2} \frac{1}{k^2} e^{-i\mathrm{k_y v_0}t}\,. \tag{7}$$

Next, the potential (6) is generalized to

$$\Phi_1 = -\frac{Gm}{\sqrt{r_0^2 + \mathrm{x}^2 + (\mathrm{y} - \mathrm{v_0}t)^2 + \mathrm{z}^2}}\,, \tag{8}$$

which corresponds to an extended body with the mass distribution of a Plummer sphere (Binney & Tremaine 1987),

$$\rho = \frac{m}{\frac{4\pi}{3} r_0^3} \left(1 + \frac{r^2}{r_0^2}\right)^{-\frac{5}{2}}\,. \tag{9}$$

The Fourier transform of a moving Plummer sphere is given by

$$\Phi_\mathbf{k} = -\frac{Gm}{2\pi^2} \frac{r_0}{k} K_1(kr_0) e^{-i\mathrm{k_y v_0}t}\,, \tag{10}$$

where K_1 denotes the modified Bessel function of the second kind. As third example we consider a perturber which has the mass density distribution of a Hernquist (1990) profile,

$$\rho = \frac{mr_0}{2\pi} \frac{1}{r(r_0 + r)^3}. \tag{11}$$

Its gravitational potential is given by

$$\Phi_1 = -\frac{Gm}{r_0 + r}\,. \tag{12}$$

The Fourier transform of a moving Hernquist sphere can be calculated using eq. (3.722) of Gradshteyn & Rhyzik (2000)[1] leading to

$$\Phi_\mathbf{k} = -\frac{Gm}{2\pi^2} \frac{1}{k^2} [1 + kr_0 \cos(kr_0)\mathrm{si}(kr_0) - kr_0 \sin(kr_0)\mathrm{ci}(kr_0)] e^{-i\mathrm{k_y v_0}t}\,, \tag{13}$$

where si and ci denote the sine- and cosine-integrals, respectively. The model of a Plummer sphere has often been used in numerical simulations of the accretion and their eventual

[1] We use the identity $\sin kr = -\frac{1}{r}\frac{\partial}{\partial k}\cos kr$ in eq. (3.722).

disruption of satellite galaxies in massive parent galaxies. Plummer spheres have constant density cores, whereas numerical simulations of the formation of galactic haloes in cold dark matter cosmology show that dark haloes may have a central density cusp (Navarro, Frenk & White 1997). Thus models of a Plummer or a Hernquist sphere should encompass the range of plausible models for satellite galaxies. The density in both models falls off radially steeper than found in the cold dark matter galaxy cosmogony simulations. This mimics the tidal truncation of satellite galaxies in the gravitational field of their parent galaxies. A more technical point is that a density profile as shallow as r^{-3} as suggested by Navarro, Frenk & White (1997) lends itself not easily to an analytic treatment, because the total mass would be diverging without an outer cut-off.

4 DYNAMICAL FRICTION

The ensemble of stars is accelerated by the moving perturber as

$$< \dot{\mathbf{v}} >= -\int d^3\mathrm{x} \int d^3\mathrm{v} f(\mathbf{x},\mathbf{v}) \nabla \Phi_1 \,, \tag{14}$$

where f denotes the full distribution function $f = f_0 + f_1$. The contribution from f_0 cancels out, and introducing the Fourier transforms (2) we find

$$< \dot{\mathbf{v}} >= -\int d^3\mathrm{x} \int d^3\mathrm{v} \int d^3\mathrm{k}\, i\mathbf{k}\Phi_{\mathbf{k}} \times e^{i[\omega t + \mathbf{k}\cdot\mathbf{x})]} \int d^3\mathrm{k}'\, f_{\mathbf{k}'} e^{i[\omega' t + \mathbf{k}'\cdot\mathbf{x}]} \,. \tag{15}$$

From symmetry reasons the acceleration vector $< \dot{\mathbf{v}} >$ is expected to be oriented along the y–axis. In eq. (15) the frequency ω, and similarly ω', is given according to eqns. (7),(10) and (13) by $\omega = -\mathrm{k_y v_0} - i\lambda$ where we have introduced following Landau's rule a negative imaginary part, which we will let go to zero in the following. Moreover, $\Phi^*_{\mathbf{k}} = \Phi_{-\mathbf{k}}$ so that the potential is a real quantity. Equation (15) simplifies to

$$< \dot{\mathbf{v}} >= (2\pi)^3 \int d^3\mathrm{v} \int d^3\mathrm{k}\, i\mathbf{k}\Phi_{-\mathbf{k}} f_{\mathbf{k}} e^{2\lambda t} \,. \tag{16}$$

Using expression (5) this can be evaluated as

$$\begin{aligned} < \dot{\mathbf{v}} >= & -\frac{(2\pi)^{5/2} n_\mathrm{b}}{\sigma^3} \int d^3\mathrm{k} \int_{-\infty}^{\infty} d\upsilon \, \frac{ik\mathbf{k}\upsilon}{-\mathrm{k_y v_0} - i\lambda + k\upsilon} \\ & \times |\Phi_{\mathbf{k}}|^2 e^{2\lambda t} e^{-\frac{\upsilon^2}{2\sigma^2}} \qquad (17) \\ = & \frac{(2\pi)^{5/2} n_\mathrm{b}}{\sigma^3} \int d^3\mathrm{k} \int_{-\infty}^{\infty} d\upsilon \, \frac{k\mathbf{k}\upsilon\lambda}{(k\upsilon - \mathrm{k_y v_0})^2 + \lambda^2} \\ & \times |\Phi_{\mathbf{k}}|^2 e^{2\lambda t} e^{-\frac{\upsilon^2}{2\sigma^2}} \,. \end{aligned}$$

Next we observe that

$$\lim_{\lambda\to 0} \; e^{2\lambda t} \frac{\lambda}{(\mathrm{k_y v_0} - k\upsilon)^2 + \lambda^2} = \pi\delta(k\upsilon - \mathrm{k_y v_0}) \tag{18}$$

so that

$$< \dot{\mathbf{v}} >= \frac{(2\pi)^{5/2}\pi n_\mathrm{b}}{\sigma^3} \int d^3\mathrm{k}\, |\Phi_{\mathbf{k}}|^2 \frac{\mathbf{k}}{k} \mathrm{k_y v_0} e^{-\frac{(\mathrm{k_y v_0})^2}{2k^2\sigma^2}} \,. \tag{19}$$

The Fourier transform of any potential with spherical symmetry depends only on $k = |\boldsymbol{k}|$. Thus it follows immediately from eq. (19) that indeed the two acceleration components

$$< \dot{\mathrm{v}}_\mathrm{x} > = < \dot{\mathrm{v}}_\mathrm{z} > = \; 0 \tag{20}$$

as anticipated from symmetry reasons. Only in the direction of motion of the perturber there is a net effect. According to Newton's third law the drag force exerted on the perturber is given by $m\dot{\mathrm{v}} = -m_\mathrm{b} < \dot{\mathrm{v}}_\mathrm{y} >$ where m_b is the mass of a background particle, so that the drag force is anti–parallel to the velocity of the perturber. In order to evaluate the integrals over the wave numbers in eq. (19) it is advantageous to switch from Cartesian form $\mathrm{k_x}, \mathrm{k_y}, \mathrm{k_z}$ to a mixed representation $\mathrm{k_y}$, $k = \sqrt{\mathrm{k_x^2} + \mathrm{k_y^2} + \mathrm{k_z^2}}$, $\arctan(\mathrm{k_x}/\mathrm{k_z})$, and we obtain for the deceleration the general result

$$\dot{\mathrm{v}} = -\frac{4\pi G^2 m m_\mathrm{b} n_\mathrm{b}}{\mathrm{v_0^2}} \left[\mathrm{erf}\left(\frac{\mathrm{v_0}}{\sqrt{2}\sigma}\right) - \sqrt{\frac{2}{\pi}} \frac{\mathrm{v_0}}{\sigma} e^{-\frac{\mathrm{v_0^2}}{2\sigma^2}} \right] \ln\Lambda \,, \tag{21}$$

where erf denotes the usual error function. The Coulomb logarithm is defined as

$$\ln\Lambda = \frac{4\pi^4}{G^2 m^2} \int_{k_\mathrm{min}}^{k_\mathrm{max}} dk \; k^3 |\Phi_\mathrm{k}|^2 \tag{22}$$

In the case of a point mass formula (7) implies $\Lambda = k_\mathrm{max}/k_\mathrm{min}$. This result was first obtained in this form by Kalnajs (1972) and is identical to Chandrasekhar's formula (Chandrasekhar 1943), if $m + m_b \approx m$. The Coulomb logarithm diverges in the familiar way both on small and large scales, i.e. at k_max^{-1} and k_min^{-1}, respectively.

The Coulomb logarithm of the dynamical friction force exerted on a Plummer sphere can be calculated by inserting eq. (10) into (22) leading to

$$\ln\Lambda = r_0^2 \int_{k_\mathrm{min}}^{\infty} dk \; k \, K_1^2(r_0 k) \,. \tag{23}$$

If the Plummer radius r_0 shrinks to zero, expression (23) changes smoothly into the Coulomb logarithm of a point mass, because $\lim_{r_0\to 0} \; r_0 K_1(k_0 k) = k^{-1}$. The integral over the square of the Bessel functions in eq. (23) can be evaluated using formula (5.54) of Gradshteyn & Rhyzik (2000),

$$\ln\Lambda = -\frac{r_0^2 k_\mathrm{min}^2}{2} \left[K_1^2(r_0 k_\mathrm{min}) - K_0(r_0 k_\mathrm{min}) K_2(r_0 k_\mathrm{min}) \right] \tag{24}$$

which is approximately

$$\ln\Lambda \approx -\frac{1}{2} - \ln(r_0 k_\mathrm{min}) \,, \tag{25}$$

in the limit of $r_0 k_\mathrm{min} \ll 1$. This modified Coulomb logarithm converges on small scales precisely as found by White (1976), but still diverges on large scales. A natural cut–off will be then the size of the stellar system under consideration.

For a perturber with the density distribution of a Hernquist profile we find a Coulomb logarithm of the form

$$\begin{aligned} \ln\Lambda = \int_{k_\mathrm{min}}^{\infty} dk \; \frac{1}{k} [& 1 + r_0 k \cos(r_0 k) \mathrm{si}(r_0 k) \\ & - r_0 k \sin(r_0 k) \mathrm{ci}(r_0 k)]^2 \,. \end{aligned} \tag{26}$$

It can be shown using the asymptotic expansions of the sine– and cosine–integrals given by Abramowitz & Stegun (1972) that the integrand in expression (26) falls off at large

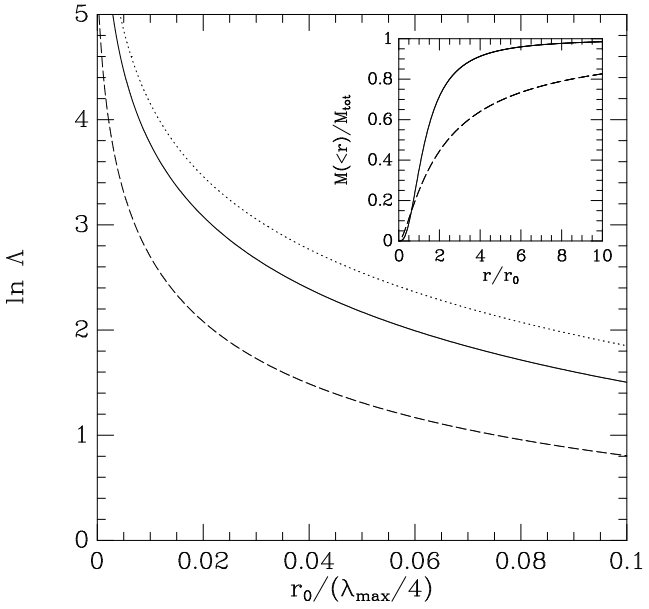

Figure 1. Coulomb logarithms of the Plummer sphere (solid line), and a sphere with a Hernquist density profile (dashed line). The dotted line indicates $-\ln(2\pi r_0/\lambda_{\max})$. r_0 denotes the radial scale lengths of the spheres and $\lambda_{\max}$ is the upper cut–off of the wavelength of the density perturbations (see text). The inlet shows the cumulative mass distributions of the Plummer and Hernquist models.

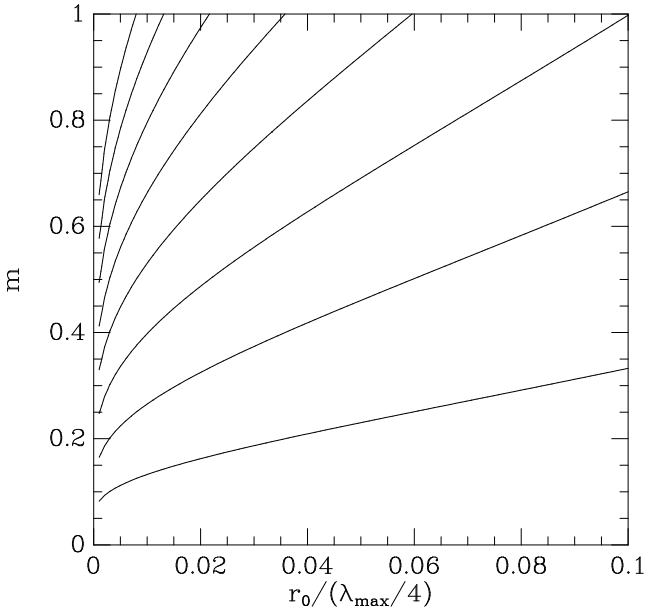

Figure 2. Contour plot of $m \cdot \ln\Lambda$ for a Plummer sphere. The mass m is given in arbitrary units. The contour levels span the rnage from 0.5 to 4 at equidistant intervals of 0.5.

k as $4r_0(r_0k)^{-5}$. Thus the Coulomb logarithm converges at small scales. This is expected because, although the density distribution has an inner density cusp, the deflecting mass 'seen' by a field star with a small impact parameter scales with square of the impact parameter. At small wave numbers a Taylor expansion shows that the square bracket in expression (26) approaches 1 so that we find a logarithmic divergence of the Coulomb logarithm as in the case of the Plummer sphere.

In Fig. 1 we illustrate the Coulomb logarithms of the Plummer sphere and a sphere with a Hernquist density distribution according to eqns. (24) and (26) as function of $r_0k_{\min}$. Fig. 1 shows clearly that at given mass small sized perturbers experience a stronger dynamical friction force than larger ones. Since the cut-off of the wave number at $k_{\min}$ is determined by the radial extent of the stellar system, which corresponds roughly to one half of the largest subtended wave length $\lambda_{\max} = 2\pi/k_{\min}$, we use actually $r_0/(\lambda_{\max}/4)$ as abscissa in Fig. 1. For comparison we have also drawn $-ln(r_0k_{\min})$ in Fig. 1. The insert shows the cumulative mass distributions of both mass models. The half mass radius of the Hernquist model measured in units of r_0 is about twice as that of the Plummer sphere. Thus for a proper comparison of the drag forces exerted on a Plummer sphere and a sphere with a Hernquist density profile the dashed line in Fig. 1 should be stretched by a factor of about 2 towards the right. But it is clear from Fig. 1 that the drag force exerted on a Plummer is always larger that the drag on a sphere with a Hernquist density profile. This is to be expected because of its shallower density profile. The logarithm $-ln(r_0k_{\min})$, although being the asymptotic expansion of the Coulomb logarithms (24) and (26) for $r_0k_{\min} \to 0$, is not a good approximation at larger $r_0k_{\min}$. There is a systematic off–set relative to the true Coulomb logarithms which is given explicitely in eq. (25) for the case of the Plummer sphere.

So far we have treated the moving perturbers as rigid bodies. In reality, perturbers can be deformed by tidal fields. One source of the tidal field is the induced polarization cloud itself. However, its effect is expected to be small. The moving perturber induces the polarization cloud in the background medium which reacts back on the perturber. Thus the dynamical friction force and any tidal fields exerted by the polarization cloud is of the order G^2 (cf. eq. 21). The deformation of the perturber can be viewed as mass excesses and deficiencies. The momentum imparted by these 'extra' masses to the particles of the background medium will be of the order of G^3 and can be safely considered as a higher order effect.

There is a further effect if the perturbers are gravitationally bound systems themselves like globular clusters or dwarf satellite galaxies. Such objects can and do loose mass due to tidal shocking. This mass loss is primarily driven by tidal shocking due to the shrinking of the tidal radii at the inner pericenters of the orbits of the perturbing objects or by disc shocking when they pass through the galactic disc (Gnedin & Ostriker 1997, Gnedin, Hernquist & Ostriker 1999). Many studies, which cannot be all enumerated here, have shown that mass loss, which reduces dynamical friction, plays thus an important role for the evolution of the orbits of the satellite galaxies. In order to illustrate the effect of mass loss, on one hand, and the effect of a finite size of the perturber, on the other hand, we show in Fig. 2 the variation of the deceleration by dynamical friction exerted on a Plummer sphere as function of the mass m and the radial scale length r_0. As can be seen from the contour plot in Fig. 2 both effects can be of comparable magnitude. If one considers, for example, a perturber with a scale length of 0.01 ($\lambda_{\max}/4$), a doubling

of its size has the same effect as a mass loss of 18 percent of the original mass.

Finally we note that our analysis can be extended in a straightforward way, to anisotropic velocity distributions of the field stars. Fuchs & Athanassoula 2005 have shown that, if the velocity ellipsoid is either prolate or oblate, the velocity dispersion in the solution of the Boltzmann equation (5) is replaced by an effective velocity dispersion which depends on the semi-axes of the velocity ellipsoid and its orientation relative to the wave vector $\mathbf{k}$. This complicates the evaluation of the integrals with respect to the wave numbers in eq. (19) considerably. We hope to address this problem in a forthcoming paper (Esquivel & Fuchs, in preparation).

5 ACKNOWLEDGEMENTS

We thank Andreas Just for useful discussions. Thanks are also due to the anonymous referee for helpful comments. O.E. gratefully acknowledges financial support by the International-Max-Planck-Research-School for Astronomy and Cosmic Physics at the University of Heidelberg.

REFERENCES

Abramowitz M., Stegun I.A., 1972, Handbook of Mathematical Functions, Dover, New York
Binney J., Tremaine S., 1987, Galactic Dynamics, Princeton University Press, Princeton
Chandrasekhar S., 1943, ApJ, 97, 255
Colpi M., Mayer L., Governato F., 1999, ApJ, 525, 720
Dekker E., 1976, Phys. Rep., 24, 315
Fuchs B., 2004, A&A, 419, 941
Fuchs B., Athanassoula E., 2005, A&A, 444, 455
Gnedin O. Y., Ostriker P. J., 1997, ApJ 474, 224
Gnedin O. Y., Hernquist L., Ostriker J.P., 1999, ApJ 514, 109
Gradshteyn I.S., Rhyzik I.M., 2000, Table of Integrals, Series, and Products, Academic Press, New York
Hénon M., 1973, in: Dynamical structure and evolution of stellar systems, G. Contopoulos, M. Hénon, D. Lynden-Bell (eds.), Lectures of the 3rd Advanced Course of the Swiss Society of Astronomy and Astrophysics, Geneva Observatory, Sauverny, p. 182
Hernquist L., 1990, ApJ, 356, 359
Kalnajs A.J., 1972, in: Gravitational N–Body Problem, M. Lecar (ed.) Reidel Publ. Comp., Dordrecht, p. 13
Lynden-Bell D., Kalnajs A.J., 1972, MNRAS, 157, 1
Marochnik L.S., 1968, SvA, 11, 873
Navarro J.F., Frenk C.S., White S.D.M., 1997, ApJ, 490, 493
Stix T.H., 1992, Waves in Plasmas, AIP, New York
Tremaine S., Weinberg M.D., 1984, MNRAS, 209, 729
White S.D.M., 1976, MNRAS, 174, 467